Feedforward and Feedback Control of a Solution Copolymerization Reactor

A control system is designed for a copolymerization reactor using a combination of feedforward, ratio, and feedback control to regulate polymer production rate, copolymer composition, molecular weight, and reactor temperature. The solution copolymerization of methyl methacrylate and vinyl acetate in a continuous stirred tank reactor is used as an illustrative example with the kinetic parameters and reactor operating conditions obtained from the literature. The process includes equipment to recycle unreacted monomers and solvent. The recycle stream introduces disturbances to the reactor feed, which perturb the polymer properties. A feedforward control strategy is proposed to counter these disturbances, and its effectiveness is demonstrated using the model. The mathematical model is used to investigate input/output control pairings in order to identify the fundamental nature of the solution copolymerization control problem and to determine the best control system structure. The combined feedforward/feedback strategy is tested on a nonlinear model of the process for set point changes and compensation of unmeasured reactor disturbances. The performance of the control system design was quite good, and such designs have been found successful in plant operations.

John P. Congalidis
John R. Richards
Polymer Products Department
E. I. du Pont de Nemours and Company
Wilmington, DE 19898

W. Harmon Ray
Department of Chemical Engineering
University of Wisconsin
Madison, WI 53706

Introduction

The manufacture of synthetic polymers is an important segment of the chemical industry with a production of over 100 billion kg annually (Ray, 1986). These polymers are produced in many different reactor types by different kinetic mechanisms, which result in complex and interesting control problems. A very important method of polymer production is free radical solution polymerization in a continuous stirred tank reactor (CSTR). Recently, as traditional homopolymer businesses have matured and differentiation of product offerings has become important, production of specialty copolymers has increased significantly. Copolymers provide unique mechanical, physical, and chemical properties for the end user.

Increased competition and emphasis on product quality have made the earlier methods of recipe control inadequate. Recipe control implies that the reactor operating conditions are updated infrequently based on product analysis from the laboratory. Improvements in control hardware and advances in control theory have provided new tools to attack the polymerization control problem. These new tools are necessary because the control of polymerization reactors is a tough and complex problem. Some of the reasons for this complexity are the paucity of on-line sensors for product quality monitoring, the extreme sensitivity of the steady state of many types of polymerization reactors to small changes in parameter values or operating conditions, and the highly interactive nonlinear dynamic behavior often exhibited by these reactors.

Recent developments in polymerization reactor control have been critically reviewed by Ray (1986) and Eliçabe and Meira (1988). An industrial perspective on reactor control has been presented by Schnelle and Richards (1986) and by Richards and Schnelle (1988). The following approaches to the control of polymerization reactors have been discussed in the literature:

• *The development of optimal trajectories for the manipulated variables.* For example Ray (1967), Ray and Gall (1969), Hicks et al. (1969), and Tsoukas et al. (1982) investigated narrowing the molecular weight distribution or the copolymer composition distribution in batch and semibatch solution polymerization reactors by manipulating temperature, monomer, and initiator addition during the batch. Manipulated-variable trajectories were generated, which transformed the control prob-

Correspondence concerning this paper should be addressed to J. P. Congalidis.

lem into an optimization problem. However, the absence of feedback from the controlled variables makes this strategy vulnerable to model inaccuracies and disturbance effects.

• *The use of nonlinear state estimation techniques to estimate infrequently measured control variables.* For example, Jo and Bankoff (1976) utilized an extended Kalman filter to obtain estimates of conversion and weight average molecular weight in an experimental solution polymerization of vinyl acetate carried out in a small glass CSTR. Schuler and Zhang (1985), at the simulation level, considered the estimation of temperature, monomer and initiator concentrations, and the first three moments of the polymer chain length distribution for the free radical polymerization of styrene. Later experimental studies (Schuler and Papadopoulou, 1986) confirmed their simulation results. Arriola and Ray (Ray, 1986) considered the question of state estimation using both on-line and off-line delayed measurements to estimate the MWD and branching distribution in a polymerization reactor.

• *The evaluation of specific feedback controllers.* For example, Kwalik (1988) used the multivariable adaptive controller of Vogel and Edgar (1988) to control the reactor monomer concentration and temperature in the solution homopolymerization of methyl methacrylate in a CSTR. Their simulations indicated acceptable performance in the presence of noise and load changes but detected difficulties, particularly in the multiple steady state region, where the interactions are stronger.

An additional complication in the control problem occurs when the unreacted monomers and solvent are recycled back to the reactor. In this case, the fresh (or make-up) feeds are the manipulated variables along with reactor jacket temperature. The recycle stream is necessary for economic reasons and occurs frequently in commercial polymer reaction processes.

In this paper, the polymerization control problem is addressed for the cases where reactor design and operation have been chosen to avoid the problems of parametric sensitivity, complex dynamics, and process runaway. The reactor operating point was, therefore, designed to be open loop stable so as to avoid controlling around an open loop unstable operating point. The control system design procedure reflects the industrial experience of the authors. Table 1 is an outline of the design methodology that was followed. A detailed nonlinear model of the reactor and the recycle system was derived from first principles. A feedforward control strategy was developed and tested on the model to counter disturbances in the recycle stream. The reactor output variables were identified as the polymer production rate, composition, molecular weight, and reactor temperature. The nonlinear model was used to identify transfer functions for various possible choices of manipulated variables. These transfer functions were used to select the appropriate feedback reactor control structures by ranking various candidate structures according to their condition number (Morari, 1983), minimum singular value (Yu and Luyben, 1986), and relative gain array (Bristol, 1966). Four proportional-integral (PI) controllers were tuned to control the reactor outputs using the selected manipulated variables. The feedback strategy was implemented hierarchically above the feedforward level. That is, the outputs from the feedback controllers are inputs to the feedforward controllers as can be seen in the subsequent discussion of Figure 1. The control performance was tested on the nonlinear model for setpoint changes and rejection of disturbances around the steady-state reactor operating point. In what follows we shall demonstrate the performance of this approach using an example solution polymerization process.

Table 1. Control System Design Methodology

Copolymerization Process Model
- Development of process nonlinear model
- Design of steady-state operating point

Feedforward Control of Recycle
- Design of feedforward controllers
- Check disturbance rejection

Feedback control of polymer properties and rate
- Obtain process and disturbance transfer functions
- Analyze control structure/pairings using singular value decomposition and relative gain array
- Obtain minimum realization linear state space model
- Tune PI controllers for setpoint changes by integration of state space model
- Check setpoint and disturbance rejection on nonlinear model

Development of Process Model

Figure 2 is a flow diagram of a copolymerization reactor with a recycle loop. Monomers A and B are continuously added with initiator, solvent, and chain transfer agent. In addition, an inhibitor may enter with the fresh feeds as an impurity. These feed streams are combined (stream 1) with the recycle stream (stream 2) and flow to the reactor (stream 3), which is assumed to be a jacketed, well-mixed tank. A coolant flows through the

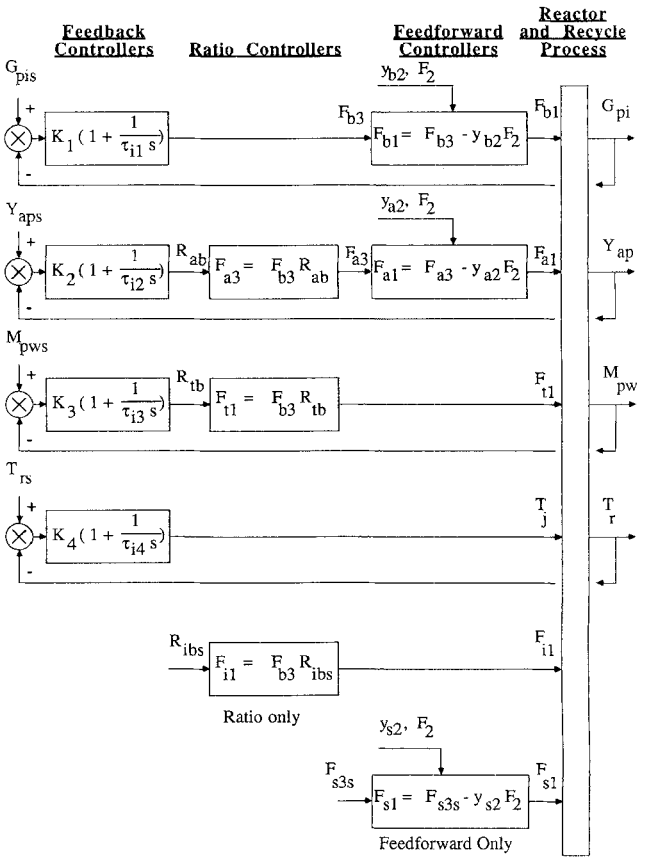

Figure 1. Control structure.

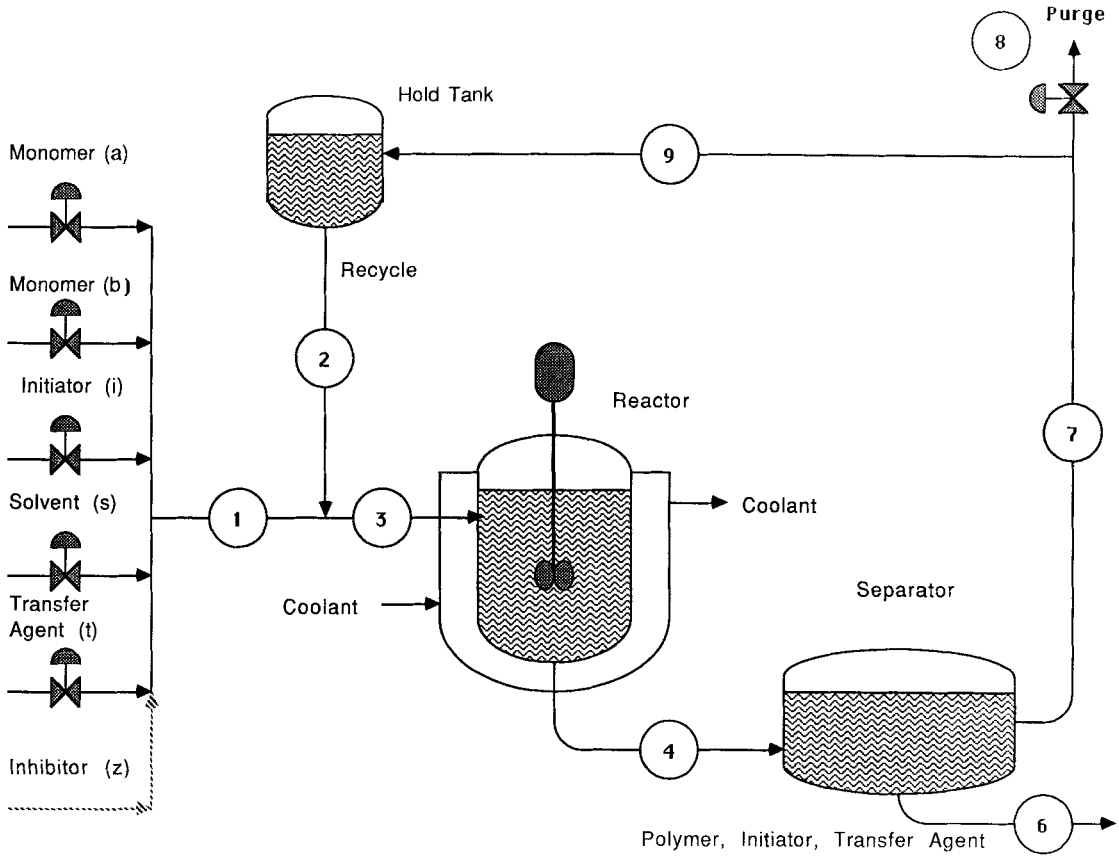

Figure 2. Copolymerization reactor with recycle.

jacket to remove the heat of polymerization. Polymer, solvent, unreacted monomers, initiator and chain transfer agent flow out of the reactor to the separator (stream 4). Here, polymer is removed from the stream (stream 6). In our study, residual initiator and chain transfer agent are also removed in this step. In actual processes, the separator often involves a series of steps which may include dryers and distillation columns. In our present example, unreacted monomers and solvent (stream 7) then continue on to a purge point (stream 8) which represents venting and other losses. Purging is required to prevent accumulation of inerts in the system. After the purge, the monomers and solvent (stream 9) are stored in the recycle hold tank which acts as a surge capacity to smooth out variations in the recycle flow and composition. The effluent (stream 2) recycle is then added to the fresh feeds.

The nonlinear mathematical model which describes the liquid-full reactor is presented in detail in the Appendix. It was assumed that a properly tuned Proportional Integral (PI) controller can be used to manipulate the coolant flow rate in order to obtain any value of the reactor jacket temperature. Therefore, in the discussion of the selection of a control structure for the reactor, the jacket temperature and not the coolant flow rate was one of the manipulated variables. The separator and hold tank are described as isothermal first-order lags with constant level and residence time equal to the reactor residence time. These assumptions eliminate the need for level controllers. In actual practice, these pieces of equipment would be subject to some inventorying and deinventorying. However, this detail was not considered important for the purposes of this paper. The purge is characterized by a constant valve setting for the ratio of stream 8 to stream 7.

In this study, monomer A is methyl methacrylate, monomer B is vinyl acetate, the solvent is benzene, the initiator is azobisisobutyronitrile (AIBN), and the chain transfer agent is acetaldehyde. The monomer stream may also contain inhibitors such as *m*-dinitrobenzene (*m*-DNB). This system is interesting, because methyl methacrylate is much more reactive than vinyl acetate in copolymerization, as indicated by their respective reactivity ratios of 26 and 0.03, although the reverse is true in homopolymerization.

The steady-state operating point was designed by the following procedure. The important reactor output variables for product quality control are the polymer production rate (G_{pi}), mole fraction of monomer A in the copolymer (Y_{ap}), weight average molecular weight (M_{pw}), and reactor temperature (T_r). The inputs are the reactor flows of monomer A (G_{af}), monomer B (G_{bf}), initiator (G_{if}), chain transfer agent (G_{tf}), solvent (G_{sf}), inhibitor (G_{zf}), the temperature of the reactor jacket (T_j), and the temperature of the reactor feed (T_{rf}). The reactor, separator, and hold tank contained at startup pure solvent preheated to 353.15 K. The inputs to the nonlinear model were then varied in order to obtain acceptable steady-state values for the output variables. The steady-state operating conditions are summarized in Table 2. Under these conditions, the reactor residence time is $\theta_r = 6$ h and the overall reactor monomer conversion is 20%. These operating conditions ensure that the viscosity of the reaction medium remains moderate. Table 2 also indicates that the temperature of the reactor feed T_{rf} is practically equal to the

Table 2. Steady-State Operating Conditions

Inputs	
Monomer A (MMA) feed rate	$G_{af} = 18$ kg/h
Monomer B (VAc) feed rate	$G_{bf} = 90$ kg/h
Initiator (AIBN) feed rate	$G_{if} = 0.18$ kg/h
Solvent (Benzene) feed rate	$G_{sf} = 36$ kg/h
Chain transfer (Acetaldehyde) feed rate	$G_{tf} = 2.7$ kg/h
Inhibitor (*m*-DNB) feed rate	$G_{zf} = 0.$
Reactor jacket temperature	$T_j = 336.15$ K
Reactor feed temperature	$T_{rf} = 353.15$ K
Purge ratio	$\xi = 0.05$
Reactor parameters	
Reactor Volume	$V_r = 1$ m^3
Reactor heat Transfer Area	$S_r = 4.6$ m^2
Outputs	
Polymer production rate	$G_{pi} = 23.3$ kg/h
Mole fraction of A in polymer	$Y_{ap} = 0.56$
Weight average molecular weight	$M_{pw} = 35{,}000$
Reactor temperature	$T_r = 353.01$ K

reactor temperature T_r, because we have chosen to simulate reactor operation with a preheated feed where the sole source of heat removal is through the jacket.

Feedforward Control of Recycle

The presence of the recycle stream introduces disturbances in the reactor feed which perturb the polymer properties. The objective of the feedforward control is to compensate for these disturbances by manipulating the fresh feeds in order to maintain constant feed composition and flow to the reactor. Feedforward control of the recycle stream allows the designer to separate the control of the reactor from the rest of the process.

The feedforward control equations were obtained by writing component material balances around the recycle addition point. That is, for each component, stream 3 = stream 1 + stream 2 (see Figure 1). For example, for monomer A this mole balance is:

$$F_{a3} = F_{a1} + y_{a2}F_2 \tag{1}$$

The symbols used in this paper are detailed in the Notation. Equation 1 is then solved for the fresh feed of monomer A since it is desired to keep the goal flow of monomer A to the reactor (F_{a3}) constant:

$$F_{a1} = F_{a3} - y_{a2}F_2 \tag{2}$$

The recycle composition (y_{a2}) is typically measured by on-line gas chromatographs (GC's) which may have significant time delays. Flow (F_2) is typically measured and controlled by manipulating the recycle valve to maintain the desired inventory in the hold tank. Any disturbances in the recycle composition (y_{a2}) or flow (F_2) will cause variations in the fresh feed in order to keep the reactor feed (F_{a3}) constant. Since only monomers A and B and solvent are present in the recycle, only these three components have feedforward control equations. As a final consideration, if Eq. 2 causes the solvent fresh feed (F_{s1}) to go nega-

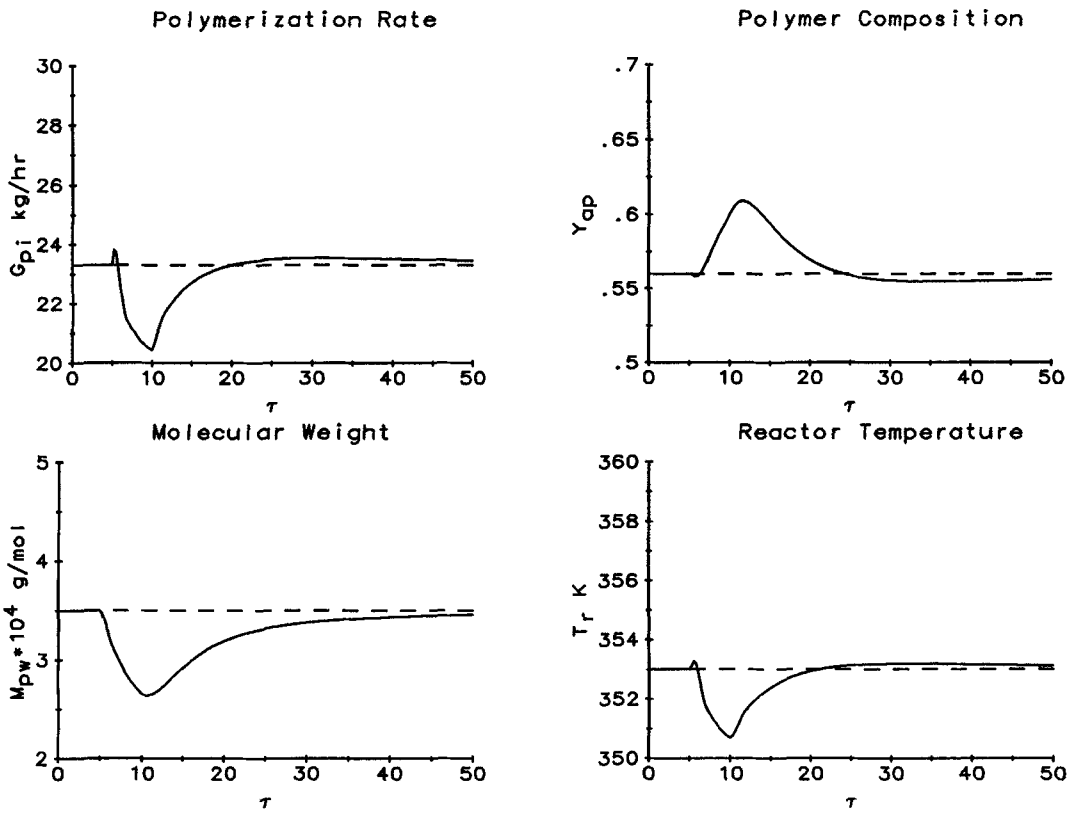

Figure 3. Open-loop output variable response to a purge disturbance.
—, output; ---, steady state

tive, the value of F_{s1} is set to zero. This case of controller output saturation will be discussed later.

The performance of the feedforward controllers is illustrated by examining the response of the output and manipulated variables to a pulse disturbance of the purge ratio that occurs while the reactor operates at steady state. This purge ratio was constant at 5% until $\tau = 5$, then increased to 30% until $\tau = 10$, and then at that point brought back to 5%. Figures 3 and 4 illustrate the open loop output and manipulated variable responses to this disturbance without any feedforward controller action. The four output variables in Figure 3 are plotted as fractions of their steady state values as indicated by a prime ('). They, therefore, approach unity at steady state. The time axis is scaled by the steady-state reactor residence time, $\tau = t/\theta_r$. The component flows are plotted as fractions of the steady-state value of the flow of that component to the reactor. The reactor jacket temperature is plotted as a fraction of its steady state value. When the purge ratio is changed the composition of the recycle stream is unaffected. However, the total recycle flowrate is changed and causes variations in the flowrates of monomers and solvent to the reactor. As shown in Figure 3, the reactor output properties vary from their steady-state values and return to their original values only after a long time ($\tau > 50$). This open loop dynamic behavior results directly from the presence of three lags in series (reactor, separator, hold tank) each of which is equal to the reactor residence time.

When the feedforward controller described above was turned on, and the same purge disturbance was introduced to the process, the reactor outputs remained absolutely constant. Figure 5 illustrates how the fresh feeds are being manipulated to maintain the composition and flows to the reactor constant throughout this disturbance. In this case, fresh solvent flow was increased and is in no danger of saturating. It should be pointed out that the flows of the initiator and of the chain transfer agent as well as the reactor jacket temperature are not being manipulated during the implementation of feedforward control. Therefore, the three curves on the bottom right half corner of Figures 4 and 5 are identical.

Design of Feedback Controllers for Polymer Properties and Production Rate

The design procedure used in this study to select a control structure is based on ranking various candidate structures according to the condition number (Morari, 1983), minimum singular value (Yu and Luyben, 1986), and relative gain array (Bristol, 1966) of the process transfer function for that specific structure. The same design procedure has been used by Levien and Morari (1987) to design multivariable controllers for distillation columns. Use of the CONSYD package of control system design programs (Holt et al., 1987) in conjunction with the nonlinear model expedited significantly this part of the design procedure.

The first issue which arises in the control design is the specification of four manipulated variables to control the four previously specified output variables. Based on engineering considerations, the selected candidates are the flows of monomer A (G_{af}), monomer B (G_{bf}), initiator (G_{if}), chain transfer agent (G_{tf}), and the reactor jacket temperature (T_j). Based on experience with polymerization processes, ratios (G_{af}/G_{bf}), (G_{if}/G_{bf}),

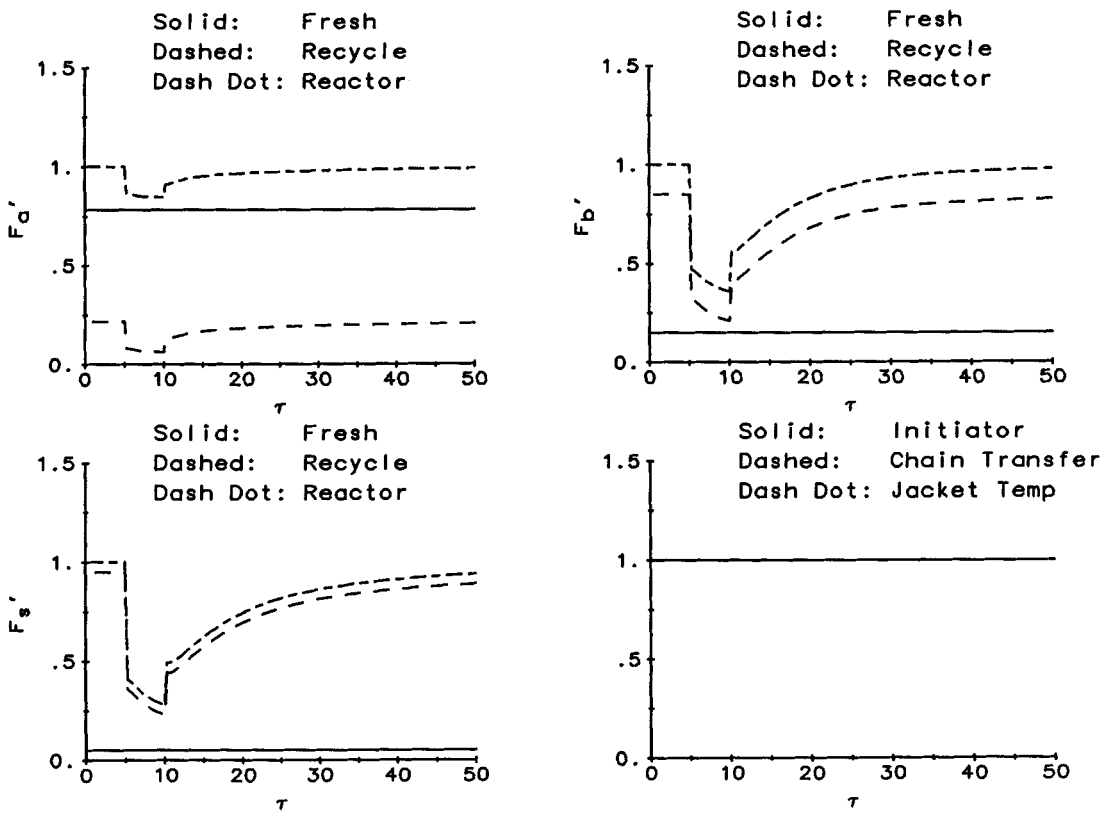

Figure 4. Open-loop, uncontrolled response of recycle flows and reactor inputs to a purge disturbance.
Variables plotted as fractions of steady-state values

Table 3. Process Transfer Function for Flow Inputs

$$\begin{bmatrix} G_{pi}^{+} \\ Y_{ap}^{+} \\ M_{pw}^{+} \\ T_{r}^{+} \end{bmatrix} = [\text{A B C D E}] \begin{bmatrix} G_{bf}^{+} \\ G_{af}^{+} \\ G_{iv}^{+} \\ T_{tf}^{+} \\ T_{j}^{+} \end{bmatrix}$$

A	B	C	D	E
$\frac{0.34063}{0.84942s+1}$	$\frac{0.20527}{0.4195s+1}$	$\frac{0.49882(0.49849s+1)}{0.12424s^2+0.40242s+1}$	0	$\frac{6.4595(0.89968s+1)}{0.065739s^2+0.29708s+1}$
$\frac{-0.41613}{2.4127s+1}$	$\frac{0.66018}{1.5098s+1}$	$\frac{-0.29677}{1.4471s+1}$	0	$\frac{-3.7235}{0.79590s+1}$
$\frac{0.29682}{2.5447s+1}$	$\frac{0.49084}{1.5443s+1}$	$\frac{-0.71493}{1.3517s+1}$	$\frac{-0.19626}{2.7110s+1}$	$\frac{-4.7145}{0.075213s^2+0.40798s+1}$
0	0	0	0	$\frac{1.0252(0.22710s+1)}{0.072732s^2+0.30978s+1}$

and (G_{tf}/G_{bf}) were chosen as additional candidates for manipulated variables.

Using the CONSYD package, step tests were performed on the nonlinear reactor model and transfer function elements were fitted by least squares to the responses of the output variables for all choices of manipulated variables. In all cases, the denominator polynomial of the transfer function was restricted to first or second order. More details are provided in the Supplemental Material. Tables 3 and 4 summarize the transfer functions obtained from this procedure. In the transfer function, elements with gains below a certain level were neglected. Inspection of Tables 3 and 4 suggests that the selection of flow ratios as manipulated variables reduces interactions among the output variables. However, more analysis was required to determine this more precisely.

Promising combinations of four manipulated variables selected from the eight candidate variables are listed in Table 5. For example, structure ABCD corresponds to columns ABCD of the transfer function matrix shown in Table 3. In order to minimize the number of realistic candidate structures, either actual flows were used as manipulated variables, or all flows were ratioed to the flow of monomer *B*.

For each of the structures of Table 5, there are 4! possible ways that the selected four manipulated variables can be paired with the four output variables. All these pairings have the same zero frequency condition number and minimum singular value. However, the diagonal elements of the relative gain array (RGA) matrix are different for each pairing indicating different degrees of steady-state interaction. Therefore, each selection of four manipulated variables was paired to the output variables in a way that yields diagonal elements in the RGA as close to unity as possible and is therefore the "best" pairing.

The remaining columns of Table 5 show the zero frequency minimum singular value and the condition number for both the original scaling of manipulated variables and the "optimal" scaling. The condition number of a matrix is defined as the ratio of its maximum singular value over its minimum singular value. For a multivariable system, the condition number and the mini-

Table 4. Process Transfer Function for Ratio Inputs

$$\begin{bmatrix} G_{pi}^{+} \\ Y_{ap}^{+} \\ M_{pw}^{+} \\ T_{r}^{+} \end{bmatrix} = [\text{F B C D E}] \begin{bmatrix} G_{bf}^{+} \\ (G_{af}/G_{bf})^{+} \\ (G_{tf}/G_{bf})^{+} \\ (G_{tf}/G_{bf})^{+} \\ T_{j}^{+} \end{bmatrix}$$

F	B	C	D	E
$\frac{0.98711(0.12011s+1)}{0.065948s^2+0.36662+1}$	$\frac{0.20527}{0.4195s+1}$	$\frac{0.49882(0.49849s+1)}{0.12424s^2+0.40242s+1}$	0	$\frac{6.4595(0.89968s+1)}{0.065739s^2+0.29708s+1}$
0	$\frac{0.66018}{1.5098s+1}$	$\frac{-0.29677}{1.4471s+1}$	0	$\frac{-3.7235}{0.79590s+1}$
$\frac{-0.16099}{0.908165s+1}$	$\frac{0.49084}{1.5443s+1}$	$\frac{-0.71493}{1.3517s+1}$	$\frac{-0.19626}{2.711s+1}$	$\frac{-4.7145}{0.075213s^2+0.40798s+1}$
0	0	0	0	$\frac{1.0252(0.22710s+1)}{0.072732s^2+0.30978s+1}$

Table 5. Analysis of Control Structure and Input/Output Pairings

Structure	Best *diag* (RGA)	Original Scaling		Optimal Scaling	
		σ_{min}	$\sigma_{max}/\sigma_{min}$	σ_{min}	$\sigma_{max}/\sigma_{min}$
ABCD	—	0.0	∞	0.0	∞
ABCE	(0.28, 0.66, 0.57, 1.0)	0.09673	92.37	0.442	5.57
ABDE	(0.72, 0.72, 1.0, 1.0)	0.01629	546.0	0.231	9.837
ACDE	(1.95, 1.95, 1.0, 1.0)	0.02575	346.6	0.1263	18.86
CBDE	(0.84, 0.84, 1.0, 1.0)	0.03765	237.3	0.3142	7.951
FBCD	—	0.0	∞	0.0	∞
FBCE	(1.24, 1.59, 1.79, 1.0)	0.1137	78.87	0.2983	8.321
FBDE	(1.0, 1.0, 1.0, 1.0)	0.09755	91.50	0.4796	4.777
FCDE	(1.0, 1.0, 1.0, 1.0)	0.03649	245.5	0.2890	8.455

mum singular value are measures of the difficulty of the control problem and the innate robustness of the dynamic system. The optimal scaling minimizes the condition number over all possible scalings and all frequencies (Morari, 1983). Figures 6 and 7 show the frequency dependence of the singular values and the condition number with original scaling for structure FBDE. These figures show that the condition number is practically constant at low frequencies but increases significantly in the high-frequency regime to indicate that the control problem becomes more difficult. All other structures showed a qualitatively similar frequency dependence.

Examination of the condition number of Table 5 shows that the two structures with the lowest condition number are FBCE and FBDE. These two structures use ratios as manipulated variables and result in superior control. The only difference between them is that in structure FBDE the ratio of chain transfer agent to monomer B is used to control molecular weight, whereas in structure FBCE the ratio of initiator to monomer B is used to control molecular weight. However, the diagonal RGA of structure FBCE indicates some steady state interactions. Although structure FBDE has a slightly higher unscaled condition number, it has smaller steady state interactions, the smallest scaled condition number, and the largest minimum singular value. Therefore it was chosen as the best structure.

After the selection of a control structure, feedback controllers were designed to control the outputs using the selected inputs as manipulated variables. Although there are many possible controllers, four single input/single output proportional integral

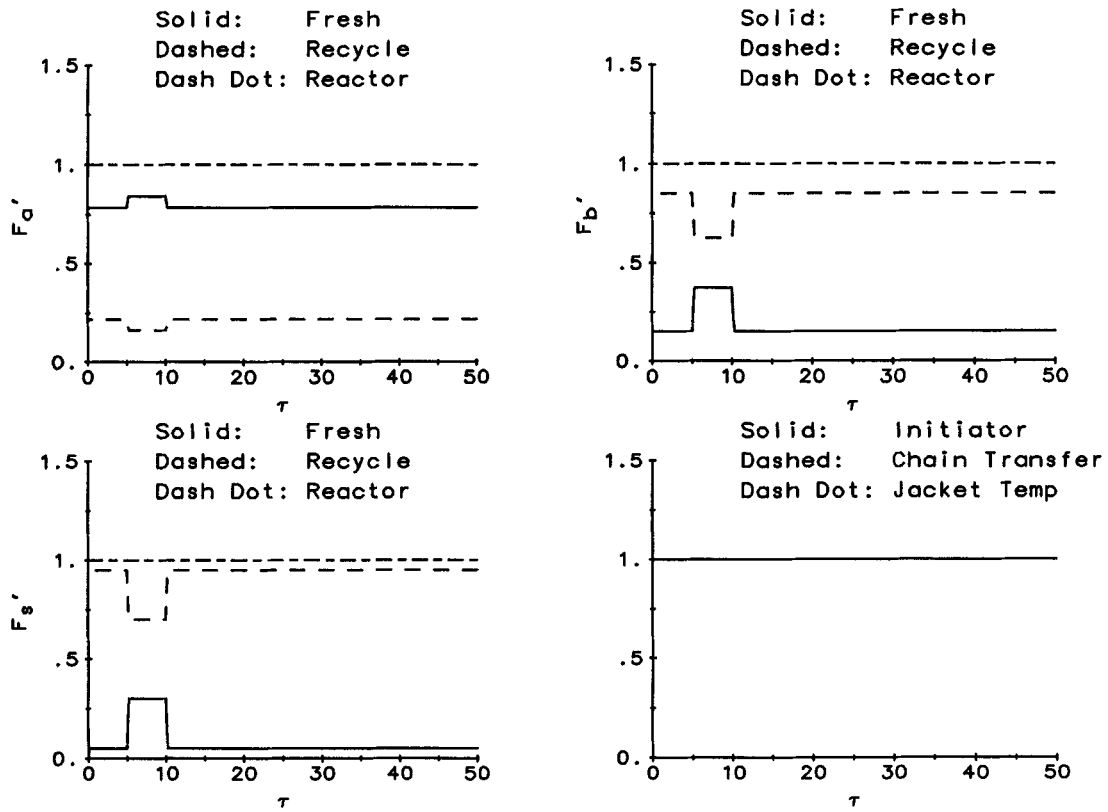

Figure 5. Response of manipulated variables to a purge disturbance.
Feedforward control is "on" and no feedback control action. Variables plotted as fractions of steady-state values.

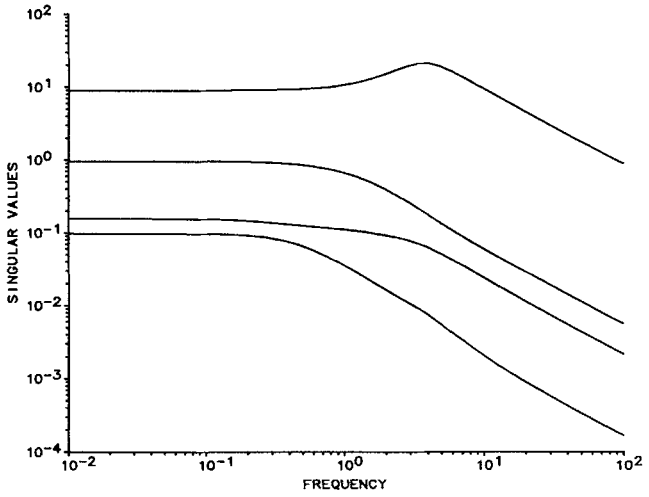

Figure 6. Frequency dependence of singular values of structure FBDE with original scaling.

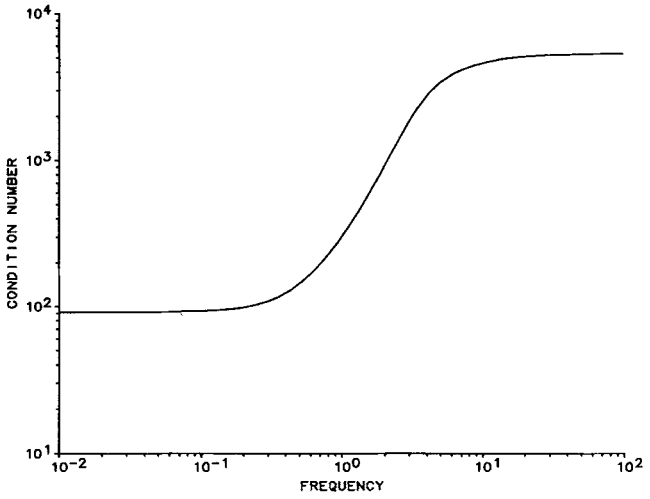

Figure 7. Frequency dependence of condition number of structure FBDE with original scaling.

Table 6. Tuning Constants for Selected Control Structure*

Manipulated	Output	K	$1/\tau_i$
G_{bf}^{+}	G_{pi}^{+}	2	4
$(G_{af}/G_{bf})^{+}$	Y_{ap}^{+}	2	1
$(G_{tf}/G_{bf})^{+}$	M_{pw}^{+}	−6	1
T_j^{+}	T_r^{+}	0.2	6

*Controller reset time τ_i is reported as a fraction of the reactor residence time.

(PI) controllers were chosen because of their simplicity. This selection does not preclude the later use of a multivariable controller if the performance of the PI controller is not satisfactory. The transfer function matrix FBDE was converted to a linear state space model using a minimal realization procedure (Holt et al., 1987). The PI controllers were tuned on the linear model by observing the output response. The interaction index proposed by Economou and Morari (1986) indicated that the temperature loop is dominant, interacts with the other loops, and

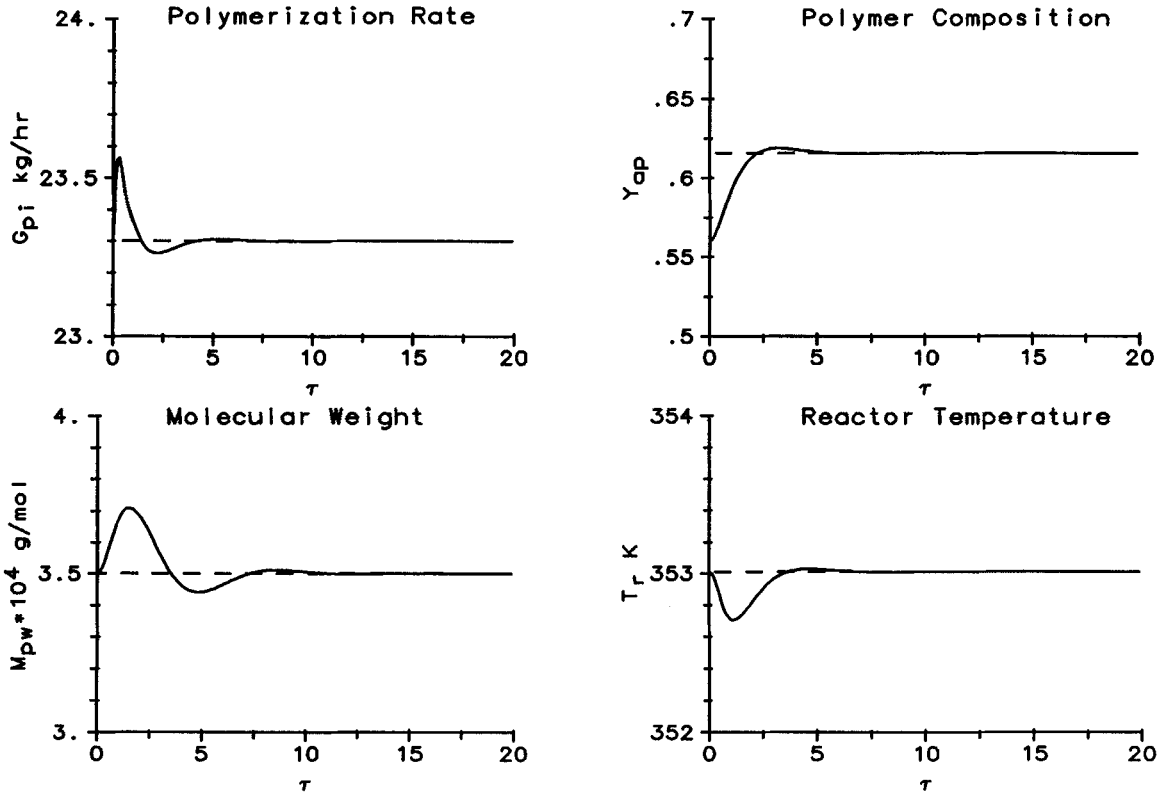

Figure 8. Response of output variables to composition setpoint change.
Feedforward and feedback control are "on" —, output; ---, setpoint

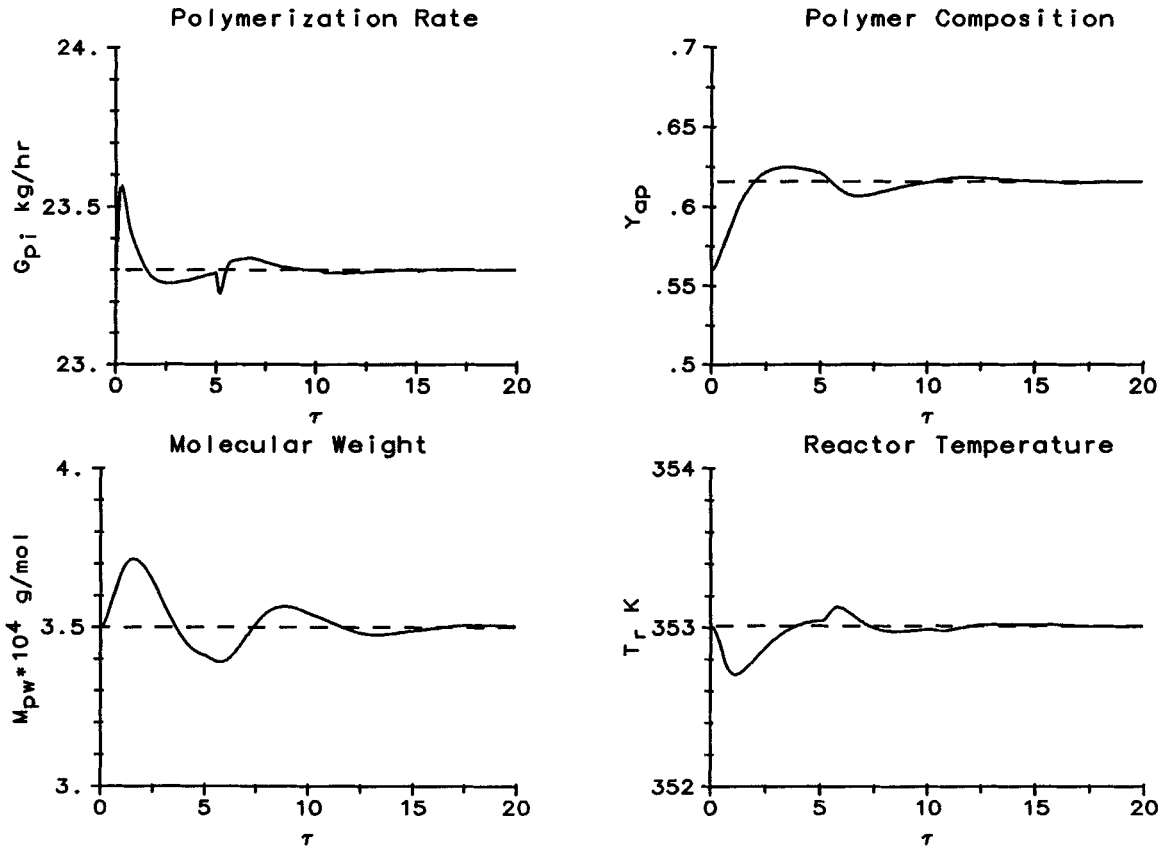

Figure 9. Response of output variables to composition setpoint change.
Feedforward and feedback control are "on," delayed GC —, output; ---, setpoint

should therefore be tuned conservatively. This interaction measure also indicated that it was possible to tune the remaining three loops tightly. Table 6 summarizes the values of the selected tuning constants.

Figure 1 is a block diagram of the combined feedforward feedback strategy. It illustrates the hierarchy of levels of control which allows each level to be tested independently for its contribution to the overall performance and leads to a more easily maintainable system in an industrial environment. As can be seen in Figure 1, the ratio controllers are implemented in the form of multiplication blocks. A more complex implementation of these ratio controllers would involve additional PI controllers with the measured ratios as controller inputs, ratio setpoints and flow outputs. Note that initiator and solvent feed rates do not have feedback action in this example.

Performance of the Control Structure on the Nonlinear Model

After preliminary testing of the control system performance using the approximate linear model, it is necessary to test the proposed control design on the complete nonlinear process model. The effect of setpoint changes for each of the four output variables was examined in detail. Space only permits a presentation of some typical results.

Figures 8 and 9 illustrate the effect of a 10% increase in the setpoint of the mole fraction of A in the polymer to simulate a polymer type or grade change. Figure 8 shows the output variable response to the composition setpoint change with feedforward and feedback control on. The performance of the system is quite good with the properties near setpoint in about 5 time units. However, the polymer molecular weight shows a more complex dynamic behavior, which is characteristic of the highly interactive dynamics of solution polymerization reactors, and reaches steady state after approximately 8 time units. This case does not include time delays in the gas chromatograph (GC) measurement of recycle composition. Our simulation also indicated that the behavior of the manipulated variables is quite acceptable in order to achieve the controller performance shown on Figure 9. For example, the jacket temperature does not vary beyond 0.2% of its steady state value to control the reactor temperature. The variation of the initiator and chain transfer flows is more significant (5% and 45% of the steady state flows respectively) but still acceptable.

Figure 9 illustrates the same setpoint change, except that a sample and hold of 5 time units has been added to the recycle GC composition measurements. This represents an enormous delay (30 hours in the present example) and the response of the system illustrated in Figure 9 has degraded significantly from that shown in Figure 8. Obviously delayed information from the GC's violates the assumption of continuous new GC information used in deriving the feedforward controllers. If the feedback controllers were not in service, this degradation of performance would occur for even shorter GC sample times. This case illustrates the robustness of the control scheme in the presence of very large measurement delays. It also shows that if the sample time is too long relative to the reactor residence time, degradation of control system performance will occur.

Figures 10 through 13 illustrate the effects of an unmeasured

impurity in the monomer feed stream that was simulated by adding to the fresh feed 0.01 part per billion inhibitor (*m*-DNB). This disturbance occurred at $\tau = 5$, after the reactor reached steady state.

Figure 10 shows the open loop output variable response to the step inhibitor disturbance without any control action at all. Even with this low inhibitor concentration the polymer properties are affected significantly. For example, the molecular weight has tripled over its steady state value. Figure 11 illustrates the futility of only controlling the reactor temperature, even with feedforward on, in the face of this powerful reactor disturbance. The reactor temperature is controlled well by the feedback controller, but the polymer properties and production rate are still affected significantly.

Figure 12 shows the output variable response and Figure 13 the manipulated variable response to the inhibitor step disturbance with both feedforward and complete feedback on. In this case the controllers bring the properties and rate back to steady state in a timely fashion. As shown in Figure 13, the solvent flow saturates, which probably causes some deterioration in the performance of the feedforward control. However, the corrective action of the feedback controllers compensates for this imperfection.

Discussion

Although these simulations indicate acceptable performance of the proposed control strategy, several issues need to be addressed before the final implementation of all levels of control in a real plant.

The experimental verification of the nonlinear reactor model is crucial in a practical implementation. The kinetic parameters used in this reactor model were obtained from the literature (Hamer et al, 1981; Brandrup and Immergut, 1975). These parameters should be fine tuned using results of experiments on a pilot or full scale reactor.

It has been assumed that accurate measurements of the output variables are continuously available for feedback control. This can be done easily for the reactor temperature but not for the remaining outputs. Periodic laboratory analysis of solution polymer concentration, polymer composition, and molecular weight are usually available, but a significant sampling deadtime is introduced. For control purposes, the required measurements can be obtained either by improved online instrumentation such as an online viscometer or a refractometer or by using a state estimator to infer the polymer properties between the measurements. The estimator can be implemented in the form of a modified Kalman filter as shown for example in the work of Ellis et al. (1988).

The startup of the reactor with the recycle stream on may be a significant problem when the goal is to minimize the amount of off-specification product and maximize production rate. For certain startup policies it may not even be possible to arrive at the desired steady state, because this reactor is characterized by multiple steady states as shown by Hamer et al. (1981). The

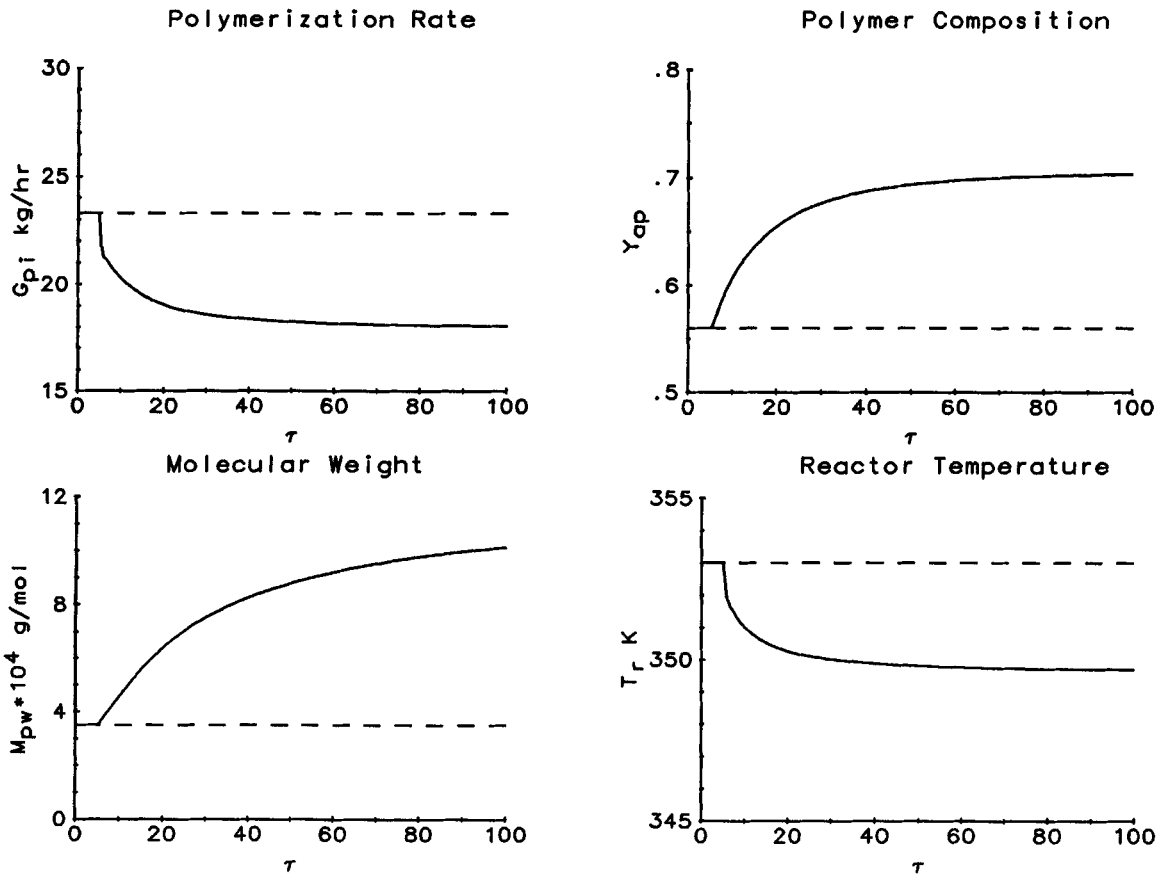

Figure 10. Open-loop output variable response to inhibitor disturbance.
—, output, ---, steady state

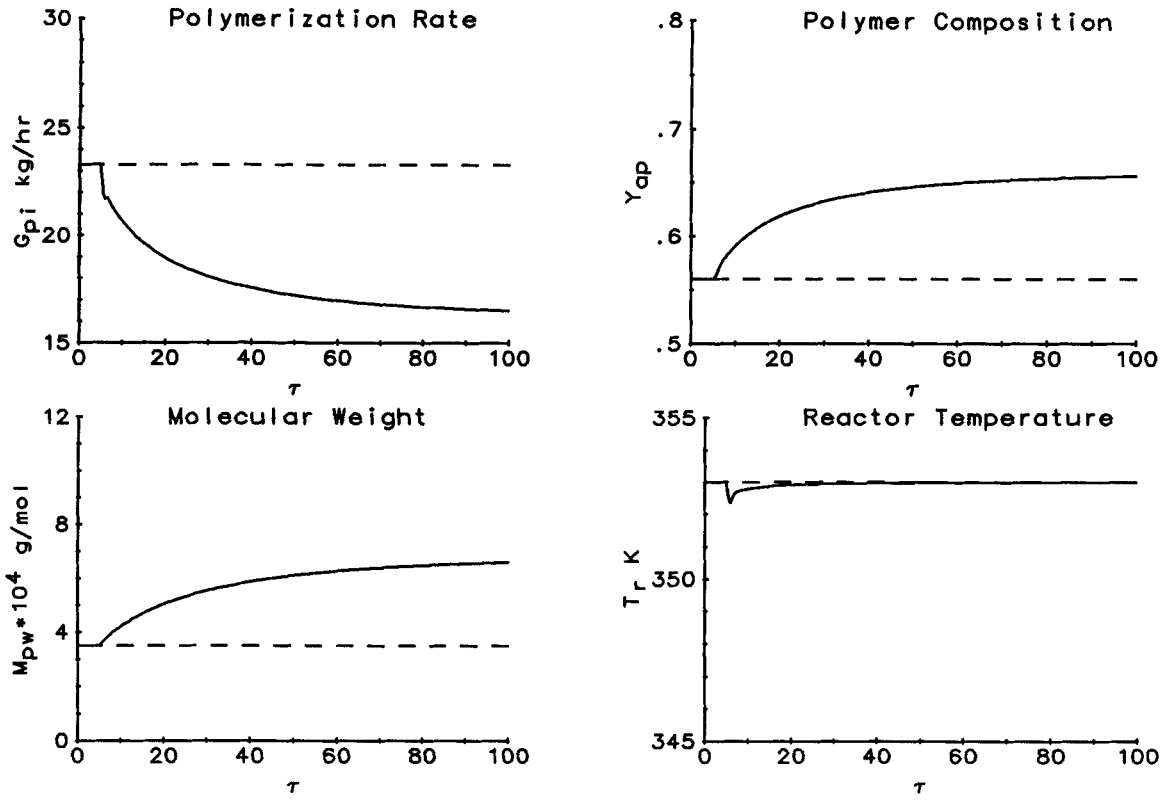

Figure 11. Response of output variables to inhibitor disturbance.
Complete feedforward, but only temperature feedback control "on" —, output; ---, setpoint

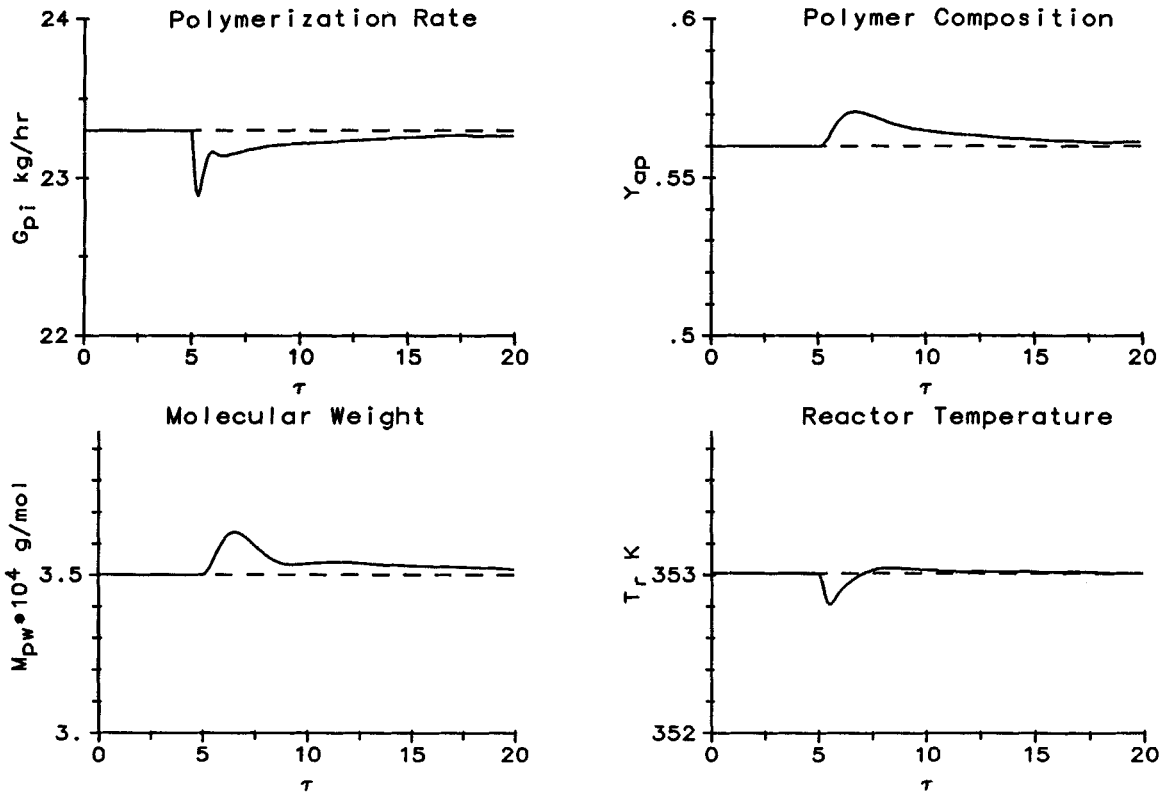

Figure 12. Response of output variables to inhibitor disturbance.
Feedforward and feedback control "on" —, output; ---, setpoint

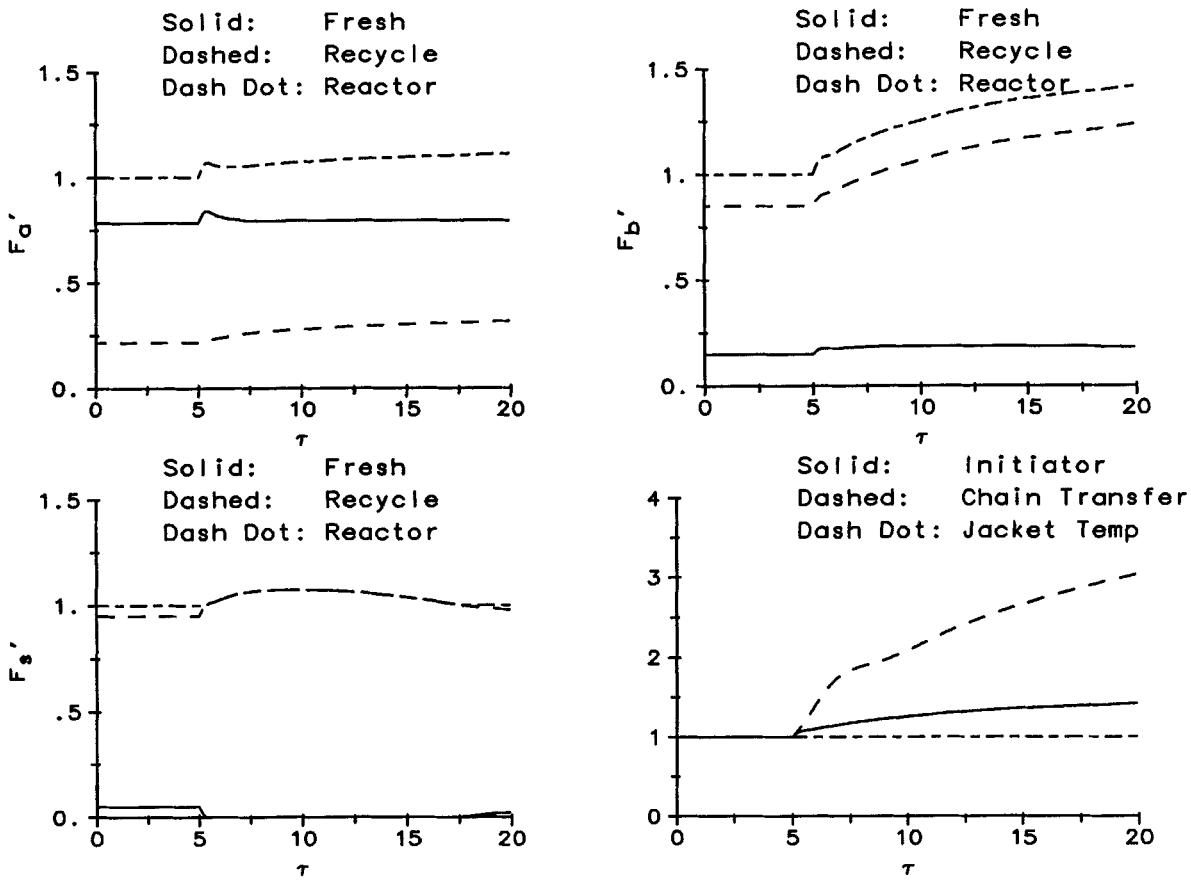

Figure 13. Response of manipulated variables to inhibitor disturbance.
Feedforward and feedback control "on." Variables plotted as fractions of steady-state values.

implementation of feedforward control during startup is discussed in the Supplemental Material.

The feedforward controllers will not operate optimally when the assumptions used in their derivation are violated. Significant delays in GC composition measurements, and errors in measurement of flow and composition will cause imperfect feedforward control. The additional complication of control valve saturation may arise when one of the fresh feeds (in this case solvent) is not consumed in the reactor. Chain transfer agent would cause a similar problem if it were not distilled from the recycle stream.

The feedback strategy used in this paper is relatively easy to implement and maintain. However, a more complex control structure (e.g., Richards and Schnelle, 1988) would be justified if further tests of this strategy indicate degradation of performance or lack of robustness. Such tests could include using a different operating point to simulate a different copolymer type or polymerization rate. A tradeoff must then be made between complexity and ease of use in the industrial environment. Distributed control systems and host computers are becoming more and more powerful and prevalent so that implementation of advanced strategies becomes feasible.

Conclusions

The problem of control of the solution polymerization process detailed in this paper has been challenging because of the complexity of the system. It has been shown that an extensive analysis using the process knowledge obtained from the mathematical model can lead to a simple, easily maintainable design. Furthermore, a hierarchical approach has been adopted so that each level of control may be tested and maintained independently. Feedforward control of the recycle stream eliminates recycle disturbances, thus separating the control of the reactor from the rest of the process. Ratio controllers on the flows to the reactor partially decouple the multivariable nature of the reactor control problem. Feedback control of polymer rate, composition, molecular weight, and reactor temperature is accomplished using PI controllers. The feedback PI and ratio controllers control the system in the face of disturbances and the nonlinear behavior of the reactor. Parts of the process control scheme described in this paper have been found successful in several plant installations.

Acknowledgment

The authors would like to thank W. D. Smith, Jr., for his encouragement and support of this work and P. D. Schnelle, Jr. and P. Harriott for helpful discussions. The authors would also like to thank J. M. Richards for her patience and support.

It is also acknowledged that the following publications are available as the Supplementary Material.

Richards, J. R., and Congalidis, J. P., "Feedforward and Feedback Control of a Copolymerization Reactor," *Proc. Amer. Cont. Conf.*, 286 (1987).

Congalidis, J. P., J. R. Richards, and W. H. Ray, "Modeling and Con-

trol of a Copolymerization Reactor," *Proc. Amer. Cont. Conf.*, 1779 (1986).

Notation

A = Arrhenius factor, monomer A
B = monomer B, Intermediate variable in MWD calculations
C = concentration, kmol/m^3
c = heat capacity, kJ/kg · K; intermediate variable in MWD calculations
E = activation energy, kJ/kmol
F = molar flow rate, kmol/s
G = mass flow rate, kg/s
H = enthalpy, kJ/kmol
I = initiator
K = controller gain
k = kinetic rate constant
L = intermediate variable in MWD calculations
M = molecular weight, kg/kmol
P = dead polymer
Q = volumetric flow rate, m^3/s
R = gas constant, kJ/kmol · K; reaction rate, kmol/m^3 · s; ratio
r = reactivity ratio
S = surface area, m^2, solvent
T = temperature, K, chain transfer agent
t = time, s
U = overall heat transfer coefficient, kJ/m^2 · s · K
V = volume, m^3
y = mole fraction
Z = inhibitor

Greek letters

α = intermediate variable in MWD calculations
γ = intermediate variable in MWD calculations
ϵ = initiator efficiency
θ = residence time, s
λ = molar concentration of monomer in polymer
ξ = molar purge fraction
ρ = density, kg/m^3
σ = singular value
τ = dimensionless time, t/θ_r; dimensionless controller reset time
χ = intermediate variable in MWD calculations
ψ = moment of molecular weight distribution

Subscripts

a = monomer A
b = monomer B
c = termination by coupling (combination)
d = termination by disproportionation
f = feed to the reactor
h = hold tank
i = initiator, instantaneous
j = cooling jacket, stream counter
k = component counter
m = number of B units in polymer chain
n = number of A units in polymer chain, number average polymer property
o = initial value
p = propagation, dead polymer
q = number of B units in polymer chain
r = reactor, number of A units in polymer chain
s = solvent, steady-state value, separator
t = chain transfer agent
w = weight average polymer property
x = chain transfer
z = inhibitor
(•) = free radical

Superscripts

(′) = variable scaled to its steady state value, e.g., $Y'_{ap} = Y_{ap}/Y_{aps}$
(+) = fractional deviation variable, e.g., $Y^{+}_{ap} = (Y_{ap} - Y_{aps})/Y_{aps}$

Appendix: Formulation of the Nonlinear Model for the Polymerization Reactor

The comprehensive solution copolymerization model used in this paper is a generalization of models that have appeared in the literature and have been verified experimentally (Hamer et al., 1981; Schmidt and Ray, 1981; Schmidt et al., 1984).

Kinetic mechanism

The following free radical kinetic mechanism is postulated for the polymerization of monomers A and B in the presence of initiator (I), solvent (S), chain transfer agent (T), and inhibitor (Z). In this mechanism $A_{n,m}\bullet$ and $B_{n,m}\bullet$ symbolize growing ("live") polymer chains containing n units of monomer A and m units of monomer B that terminate in A and B, respectively. $P_{n,m}$ represents a "dead" polymer chain containing n units of monomer A and m units of monomer B. In the calculation of the cross termination rate constants it has been assumed that:

$$k_{cab} = \sqrt{k_{caa}\,k_{cbb}}$$

$$k_{dab} = \sqrt{k_{daa}\,k_{dbb}}$$

Initiation

$$I \xrightarrow{k_i} 2I\bullet$$

$$I\bullet + A \xrightarrow{k_{ia}} A_{1,0}\bullet$$

$$I\bullet + B \xrightarrow{k_{ia}} B_{0,1}\bullet$$

$$S\bullet + A \xrightarrow{k_{is}} A_{1,0}\bullet$$

$$S\bullet + B \xrightarrow{k_{is}} B_{0,1}\bullet$$

$$T\bullet + A \xrightarrow{k_{it}} A_{1,0}\bullet$$

$$T\bullet + B \xrightarrow{k_{it}} B_{0,1}\bullet$$

Propagation

$$A_{n,m}\bullet + A \xrightarrow{k_{paa}} A_{n+1,m}\bullet$$

$$A_{n,m}\bullet + B \xrightarrow{k_{pab}} B_{n,m+1}\bullet$$

$$B_{n,m}\bullet + A \xrightarrow{k_{pba}} A_{n+1,m}\bullet$$

$$B_{n,m}\bullet + B \xrightarrow{k_{pbb}} B_{n,m+1}\bullet$$

Termination by coupling

$$A_{n,m}^{\bullet} + A_{r,q}^{\bullet} \xrightarrow{k_{caa}} P_{n+r,m+q}$$

$$A_{n,m}^{\bullet} + B_{r,q}^{\bullet} \xrightarrow{k_{cab}} P_{n+r,m+q}$$

$$B_{n,m}^{\bullet} + B_{r,q}^{\bullet} \xrightarrow{k_{cbb}} P_{n+r,m+q}$$

Termination by disproportionation

$$A_{n,m}^{\bullet} + A_{r,q}^{\bullet} \xrightarrow{k_{daa}} P_{n,m} + P_{r,q}$$

$$A_{n,m}^{\bullet} + B_{r,q}^{\bullet} \xrightarrow{k_{dab}} P_{n,m} + P_{r,q}$$

$$B_{n,m}^{\bullet} + B_{r,q}^{\bullet} \xrightarrow{k_{dbb}} P_{n,m} + P_{r,q}$$

Chain transfer to solvent

$$A_{n,m}^{\bullet} + S \xrightarrow{k_{xas}} P_{n,m} + S^{\bullet}$$

$$B_{n,m}^{\bullet} + S \xrightarrow{k_{xbs}} P_{n,m} + S^{\bullet}$$

Chain transfer to monomer

$$A_{n,m}^{\bullet} + A \xrightarrow{k_{xaa}} P_{n,m} + A_{1,0}^{\bullet}$$

$$A_{n,m}^{\bullet} + B \xrightarrow{k_{xab}} P_{n,m} + B_{0,1}^{\bullet}$$

$$B_{n,m}^{\bullet} + A \xrightarrow{k_{xba}} P_{n,m} + A_{1,0}^{\bullet}$$

$$B_{n,m}^{\bullet} + B \xrightarrow{k_{xbb}} P_{n,m} + B_{0,1}^{\bullet}$$

Chain transfer to agent

$$A_{n,m}^{\bullet} + T \xrightarrow{k_{xat}} P_{n,m} + T^{\bullet}$$

$$B_{n,m}^{\bullet} + T \xrightarrow{k_{xbt}} P_{n,m} + T^{\bullet}$$

Inhibition

$$A_{n,m}^{\bullet} + Z \xrightarrow{k_{za}} P_{n,m}$$

$$B_{n,m}^{\bullet} + Z \xrightarrow{k_{zb}} P_{n,m}$$

Each of these kinetic rate constants is computed by an Arrhenius expression of the form:

$$k = Ae^{(-E/RT_r)} \tag{1}$$

Values for the Arrhenius factor A and the activation energy E are given in Table 7. These rate constants were not corrected for the gel effect which becomes important at high reactor monomer conversions.

Material and energy balances

Assuming that the copolymerization occurs in a continuous stirred tank reactor (CSTR) with no volume change in the reacting mixture, the following mole balances can be written for

Table 7. Kinetic and Thermodynamic Parameters for Nonlinear Model

Kinetic Parameters

ϵ	1
A_i	4.5×10^{14} 1/s
A_{caa}	4.209×10^{11} m³/kmol · s
A_{cbb}	1.61×10^{9} "
A_{daa}	0 "
A_{dbb}	0 "
A_{paa}	3.207×10^{6} "
A_{pab}	1.233×10^{5} "
A_{pba}	2.103×10^{8} "
A_{pbb}	6.308×10^{6} "
A_{xaa}	32.08 "
A_{xab}	1.234 "
A_{xas}	86.6 "
A_{xat}	2,085.0 "
A_{xba}	5.257×10^{4} "
A_{xbb}	1,577 "
A_{xbs}	1,514 "
A_{xbt}	4.163×10^{5} "
A_{za}	2.2 "
A_{zb}	1.13×10^{5} "
E_i	1.25×10^{5} kJ/kmol
E_{caa}	2.69×10^{4} "
E_{cbb}	4.00×10^{3} "
E_{daa}	0.0
E_{dbb}	0.0
E_{paa}	2.42×10^{4} "
E_{pab}	2.42×10^{4} "
E_{pba}	1.80×10^{4} "
E_{pbb}	2.42×10^{4} "
E_{xaa}	2.42×10^{4} "
E_{xab}	2.42×10^{4} "
E_{xas}	2.42×10^{4} "
E_{xat}	2.42×10^{4} "
E_{xba}	1.80×10^{4} "
E_{xbb}	1.80×10^{4} "
E_{xbs}	1.80×10^{4} "
E_{xbt}	2.42×10^{4} "
E_{za}	0.0
E_{zb}	0.0

Thermodynamic Parameters

$-\Delta H_{paa}$	54.0×10^{3} kJ/kmol
$-\Delta H_{pba}$	54.0×10^{3} kJ/kmol
$-\Delta H_{pab}$	86.0×10^{3} kJ/kmol
$-\Delta H_{pbb}$	86.0×10^{3} kJ/kmol
ρr	8.79×10^{2} kg/m³
Cr	2.01 kJ/kg · K
U_r	6.0×10^{-2} kJ/m² · s · K

the monomers, the initiator, the solvent, the chain transfer agent, and the inhibitor:

$$\frac{dC_k}{dt} = \frac{C_{kf} - C_k}{\theta_r} - R_k \tag{2}$$

$$C_k(0) = C_{k0}$$

$$k = a, b, i, s, t, z$$

The reactor feed volumetric flow rate, concentrations, and reactor residence time are calculated by the following equations:

$$Q_f = \sum_k \frac{F_{kf} M_k}{\rho_r} \tag{2.1}$$

$$C_{kf} = \frac{F_{kf}}{Q_f} \tag{2.2}$$

$$\theta_r = \frac{V_r}{Q_f} \tag{2.3}$$

These mole balances are coupled with the following reactor energy balance:

$$\frac{dT_r}{dt} = \frac{T_{rf} - T_r}{\theta_r} + \frac{(-\Delta H_{paa})k_{paa}C_aC_{a\bullet} + (-\Delta H_{pba})k_{pba}C_aC_{b\bullet}}{\rho_r c_r} + \frac{(-\Delta H_{pab})k_{pab}C_bC_{a\bullet} + (-\Delta H_{pbb})k_{pbb}C_bC_{b\bullet}}{\rho_r c_r} - \frac{U_r S_r (T_r - T_j)}{V_r \rho_r c_r} \quad T_r(0) = T_{r0} \tag{3}$$

The Long chain hypothesis (Ray, 1972) results in the following expressions for the reaction rates:

$$R_a = \{(k_{paa} + k_{xaa})C_{a\bullet} + (k_{pba} + k_{xba})C_{b\bullet}\}C_a \tag{4}$$

$$R_b = \{(k_{pbb} + k_{xbb})C_{b\bullet} + (k_{pab} + k_{xab})C_{a\bullet}\}C_b \tag{5}$$

$$R_i = k_i C_i \tag{6}$$

$$R_s = (k_{xas}C_{a\bullet} + k_{xbs}C_{b\bullet})C_s \tag{7}$$

$$R_t = (k_{xat}C_{a\bullet} + k_{xbt}C_{b\bullet})C_t \tag{8}$$

$$R_z = (k_{za}C_{a\bullet} + k_{zb}C_{b\bullet})C_z \tag{9}$$

The instantaneous polymerization rate G_{pi} is therefore:

$$G_{pi} = R_aM_a + R_bM_b \tag{10}$$

Using the quasisteady-state assumption (Ray, 1972), the following expressions can be derived for the total reactor concentrations of free radicals terminating in A or B:

$$C_{a\bullet} = \frac{-l_2 + \sqrt{l_2^2 - 4l_1l_3}}{2l_1} \tag{11}$$

$$C_{b\bullet} = \beta C_{a\bullet} \tag{12}$$

In Eqs. 11 and 12, the following intermediate variables are defined:

$$\beta = \frac{(k_{pab} + k_{xab})C_b}{(k_{pba} + k_{xba})C_a} \tag{13}$$

$$l_1 = k_{caa} + k_{daa} + 2\beta(k_{cab} + k_{dab}) + \beta^2(k_{cbb} + k_{dbb}) \tag{14}$$

$$l_2 = C_z(k_{za} + \beta k_{zb}) \tag{15}$$

$$l_3 = -2k_iC_i\epsilon \tag{16}$$

Dead copolymer composition

The following mole balances can be written for the calculation of the molar concentrations of the two monomers in the dead polymer:

$$\frac{d\lambda_a}{dt} = \frac{\lambda_{af} - \lambda_a}{\theta_r} + R_a \quad \lambda_a(0) = \lambda_{a0} \tag{17}$$

$$\frac{d\lambda_b}{dt} = \frac{\lambda_{bf} - \lambda_b}{\theta_r} + R_b \quad \lambda_b(0) = \lambda_{b0} \tag{18}$$

The mole fraction of monomer A in dead polymer is calculated as follows:

$$y_{ap} = \frac{\lambda_a}{\lambda_a + \lambda_b} \tag{19}$$

Number and weight average molecular weight

In the first part of this section the computation of the zeroth, first, and second moments of the molecular weight distribution (MWD) of the "dead" (not growing) copolymer is outlined. These moments are defined as follows for $k = 0, 1, \ldots, \infty$:

$$\psi_k^p = \sum_{n=0}^{\infty}\sum_{m=0}^{\infty}(nM_a + mM_b)^k P_{n,m} \tag{20}$$

In the second part of this section, these moments are related to the moments of the MWD of the "live" (growing) copolymer, which are defined as follows for $k = 0, 1, \ldots, \infty$:

$$\psi_k^a = \sum_{n=0}^{\infty}\sum_{m=0}^{\infty}(nM_a + mM_b)^k A_{n,m\bullet} \tag{21}$$

$$\psi_k^b = \sum_{n=0}^{\infty}\sum_{m=0}^{\infty}(nM_a + mM_b)^k B_{n,m\bullet} \tag{22}$$

The number average and weight average molecular weights of the dead copolymer are then computed by the following relationships:

$$M_{pn} = \frac{\psi_1^p}{\psi_0^p} \tag{23}$$

$$M_{pw} = \frac{\psi_2^p}{\psi_1^p} \tag{24}$$

Moments of the MWD of the dead copolymer

It is necessary to specify the reactor of interest in order to calculate the moments of the MWD for the "dead" or stable polymer (CSTR for this work). Using the generating function technique, the following dynamic equations are derived as in Tsoukas et al. (1982):

$$\frac{d\psi_0^p}{dt} = \frac{\psi_{0f}^p - \psi_0^p}{\theta_r} + \frac{1}{2}k_{caa}(\psi_0^{a\bullet})^2 + k_{cab}\psi_0^{a\bullet}\psi_0^{b\bullet} + \frac{1}{2}k_{cbb}(\psi_0^{b\bullet})^2 + L_1\psi_0^{a\bullet} + L_2\psi_0^{b\bullet} \tag{25}$$

$$\frac{d\psi_1^p}{dt} = \frac{\psi_{1f}^p - \psi_1^p}{\theta_r} + k_{caa}\psi_0^{a\bullet}\psi_1^{a\bullet} + k_{cab}(\psi_0^{a\bullet}\psi_1^{b\bullet} + \psi_0^{b\bullet}\psi_1^{a\bullet}) + k_{cbb}\psi_0^{b\bullet}\psi_1^{b\bullet} + L_1\psi_1^{a\bullet} + L_2\psi_0^{b\bullet} \tag{26}$$

$$\frac{d\psi_2^p}{dt} = \frac{\psi_{2f}^p - \psi_2^p}{\theta_r} + k_{caa}\{(\psi_1^{a\bullet})^2 + \psi_0^{a\bullet}\psi_2^{a\bullet}\} + k_{cab}(2\psi_1^{a\bullet}\psi_1^{b\bullet} + \psi_2^{b\bullet}\psi_0^{a\bullet} + \psi_2^{a\bullet}\psi_0^{b\bullet}) + k_{cbb}\{(\psi_1^{b\bullet})^2 + \psi_0^{b\bullet}\psi_2^{b\bullet}\} + L_1\psi_1^{a\bullet} + L_2\psi_1^{b\bullet} \tag{27}$$

$$\psi_0^p(0) = \psi_{0o}^p,$$
$$\psi_1^p(0) = \psi_{1o}^p,$$
$$\psi_2^p(0) = \psi_{2o}^p, \tag{28}$$

In these equations the intermediate variables L_1 and L_2 are defined as follows:

$$L_1 = k_{xas}C_s + k_{xaa}C_a + k_{xab}C_b + k_{xat}C_t + k_{za}C_z + k_{daa}C_{a\bullet} + k_{dab}C_{b\bullet} \tag{29}$$

$$L_2 = k_{xbs}C_s + k_{xbb}C_b + k_{xba}C_a + k_{xbt}C_t + k_{zb}C_z + k_{dbb}C_{b\bullet} + k_{dab}C_{a\bullet} \tag{30}$$

Moments of the MWD of the live copolymer

The method of generating functions is used for this calculation (Ray, 1971a,b). These moments are the same for all reactors and only depend on the local reaction environment. The Symbolic Manipulation System MACSYMA has been used to implement this method and to derive the following analytical expressions for the zeroth, first, and second moments of the live copolymer MWD:

$$\psi_0^{a\bullet} = \frac{B_3}{B_1} \tag{31}$$

$$\psi_1^{a\bullet} = \frac{\alpha_1\alpha_2V_1(M_b + M_a) + \alpha_1c_1M_a}{B_1} - \frac{B_2B_3}{B_1^2} \tag{32}$$

$$\psi_2^{a\bullet} = \frac{-B_3\{(\alpha_1 + \alpha_2)M_aM_b + B_2(M_a + M_b - 1)\}}{B_1^2} + \frac{\alpha_1\alpha_2V_1(M_a + M_b - 1)(M_a + M_b)}{B_1} + \frac{\alpha_1c_1M_a(M_a - 1)}{B_1} + \frac{2B_2^2B_3}{B_1^3} + \psi_1^{a\bullet} - \frac{2B_2\{\alpha_1\alpha_2V_1(M_a + M_b) + \alpha_1c_1M_a\}}{B_1^2} \tag{33}$$

$$\psi_0^{b\bullet} = \frac{B_4}{B_1} \tag{34}$$

$$\psi_1^{b\bullet} = \frac{\alpha_1\alpha_2V_2(M_b + M_a) + \alpha_2c_4M_b}{B_1} - \frac{B_2B_4}{B_1^2} \tag{35}$$

$$\psi_2^{b\bullet} = \frac{-B_4\{(\alpha_1 + \alpha_2)M_aM_b + B_2(M_a + M_b - 1)\}}{B_1^2} + \frac{\alpha_1\alpha_2V_2(M_a + M_b - 1)(M_a + M_b)}{B_1} + \frac{\alpha_2c_4M_b(M_b - 1)}{B_1} + \frac{2B_2^2B_4}{B_1^3} + \psi_1^{b\bullet} - \frac{2B_2\{\alpha_1\alpha_2V_2(M_a + M_b) + \alpha_2c_4M_b\}}{B_1^2} \tag{36}$$

The following combinations of kinetic parameters are used in Eqs. 31 to 36:

$$\alpha_1 = \frac{k_{paa}C_a}{\{(k_{caa} + k_{daa})C_{a\bullet} + (k_{cab} + k_{dab})C_{b\bullet} + (k_{paa} + k_{xaa})C_a + (k_{pab} + k_{xab})C_b + k_{xat}C_t + k_{xas}C_s + k_{za}C_z\}} \tag{37}$$

$$\alpha_2 = \frac{k_{pbb}C_b}{\{(k_{cbb} + k_{dbb})C_{b\bullet} + (k_{cab} + k_{dab})C_{a\bullet} + (k_{pbb} + k_{xbb})C_b + (k_{pba} + k_{xba})C_a + k_{xbt}C_t + k_{xbs}C_s + k_{zb}C_z\}} \tag{38}$$

$$c_1 = \frac{2k_f\epsilon C_i + C_s(k_{xas}C_{a\bullet} + k_{xbs}C_{b\bullet})}{k_{paa}(C_a + C_b)} + \frac{C_t(k_{xat}C_{a\bullet} + k_{xbt}C_{b\bullet})}{k_{paa}(C_a + C_b)} + \frac{(k_{xaa}C_{a\bullet} + k_{xba}C_{b\bullet})}{k_{paa}} \tag{39}$$

$$c_4 = \frac{2k_f\epsilon C_i + C_s(k_{xas}C_{a\bullet} + k_{xbs}C_{b\bullet})}{k_{pbb}(C_a + C_b)} + \frac{C_t(k_{xat}C_{a\bullet} + k_{xbt}C_{b\bullet})}{k_{pbb}(C_a + C_b)} + \frac{(k_{xbb}C_{b\bullet} + k_{xab}C_{a\bullet})}{k_{pbb}} \tag{40}$$

$$r_1 = \frac{k_{paa}}{k_{pab}} \tag{41}$$

$$r_2 = \frac{k_{pbb}}{k_{pba}} \tag{42}$$

$$\gamma = \frac{k_{pba}}{k_{pab}} \tag{43}$$

$$c_2 = c_4 r_2 \gamma \tag{44}$$

$$c_3 = \frac{c_1 r_1}{\gamma} \tag{45}$$

$$x = \frac{1}{r_1 r_2} \tag{46}$$

$$V_1 = c_2 x - c_1 \tag{47}$$

$$V_2 = c_3 x - c_4 \tag{48}$$

$$B_1 = 1 - (\alpha_1 + \alpha_2) + \alpha_1\alpha_2(1 - x) \tag{49}$$

$$B_2 = (M_a + M_b)(1 - x)\alpha_1\alpha_2 - \alpha_1 M_a - \alpha_2 M_b \tag{50}$$

$$B_3 = \alpha_1 c_1 + \alpha_1\alpha_2 V_1 \tag{51}$$

$$B_4 = \alpha_2 c_4 + \alpha_1\alpha_2 V_2 \tag{52}$$

Separator and hold tank balances

These pieces of equipment are modeled as first-order lags on the species concentrations with constant level:

$$\frac{dC_{ks}}{dt} = \frac{C_{ksf} - C_{ks}}{\theta_s} \tag{53}$$

$$C_{ks}(0) = C_{kso}, \quad k = a, b, i, s, t, z \tag{54}$$

$$\frac{dC_{kh}}{dt} = \frac{C_{khf} - C_{kh}}{\theta_h} \tag{55}$$

$$C_{kh}(0) = C_{kho}, \quad k = a, b, i, s, t, z \tag{56}$$

Equations 1 to 56 form a system of nonlinear ordinary differential and algebraic equations that are integrated numerically using a fifth- and sixth-order Runge-Kutta algorithm. This integration allows the computation of both dynamic and steady state values for the polymerization rate, reactor temperature, copolymer composition, and molecular weight.

Literature Cited

Brandrup, J., and E. H. Immergut, eds., *Polymer Handbook*, 2nd ed., Wiley (1975).

Bristol, E. H., "On a New Measure of Interaction for Multivariable Process Control," *IEEE Trans. on Automatic Control*, **AC-11**, 133 (1966).

Economou, C., and M. Morari, "Internal Model Control: IV. Multiloop Design," *Ind. Eng. Chem. Process Des. Dev.*, **25**, 411 (1986).

Eliçabe, G. E., and G. R. Meira, "Estimation and Control in Polymerization Reactors. A Review," *Polym. Eng. and Sci.*, **28**, 121 (1988).

Ellis, M. F., V. González, T. W. Taylor, and K. F. Jensen, "Estimation of the Molecular Weight Distribution in a Batch Polymerization," *AIChE J.*, **34**, 1341 (1988).

Hamer, J. W., T. A. Akramov, and W. H. Ray, "The Dynamic Behavior of Continuous Polymerization Reactors: II. Nonisothermal Solution Homopolymerization and Copolymerization in a CSTR," *Chem. Eng. Sci.*, **36**, 1897 (1981).

Hicks, J. M., A. Mohan, and W. H. Ray, "The Optimal Control of Polymerization Reactors," *Can. J. Chem. Eng.*, **47**, 590 (1969).

Holt, B. R., N. F. Jerome, U. Buck, M. Dubinsky, C. Economou, W. Grimm, A. Galimidi, P. Grosdidier, K. Jordan, R. Klewin, W. Kraemer, G. V. Kuguenko, J. Mandler, A. Ness, T. A. Ninman, T. Plocher, D. E. Rivera, R. Sela, Z. Szakaly, H. H. Tung, C. Webb, E. Zafiriou, M. Morari, and W. H. Ray, "CONSYD-Integrated Software for Computer Aided Control System Design and Analysis," *Comput. Chem. Eng.*, **11**(2), 187 (1987).

Jo, J. H., and S. G. Bankoff, "Digital Monitoring and Estimation of Polymerization Reactors," *AIChE J.*, **22**, 361 (1976).

Kwalik, K. M., "Bifurcation Characteristics in Closed-Loop Polymerization Reactors," Diss., Georgia Institute of Technology, available from University Microfilms (1988).

Levien, K. L., and M. Morari, "Internal Model Control of Coupled Distillation Columns," *AIChE J.*, **33**(1) 83 (1987).

Morari, M., "Design of Resilient Processing Plants: III. A General Framework for Assessment of Dynamic Resilience," *Chem. Eng. Sci.*, **38**, 1881 (1983).

Ray, W. H., and C. E. Gall, "The Control of Copolymer Composition Distributions in Batch and Tubular Reactors," *Macrom.*, **2**, 425 (1969).

Ray, W. H., "Modelling Polymerization Reactors with Applications to Optimal Design," *Can. J. Chem. Eng.*, **45**, 356 (1967).

Ray, W. H., "Molecular Weight Distributions in Copolymer Systems. I. Living Copolymers," *Macrom.*, **4**, 162 (1971a).

Ray, W. H., T. L. Douglas, and E. W. Godsalve, "Molecular Weight Distributions in Copolymer Systems: II. Free Radical Copolymerization," *Macrom.*, **4**, 166 (1971b).

Ray, W. H., "On the Mathematical Modeling of Polymerization Reactors," *J. Macrom. Sci.-Revs. Macrom. Chem.*, **C8**, 1 (1972).

Ray, W. H., "Polymerization Reactor Control," *IEEE Control Systems Mag.*, **6**(4)S, 3 (1986).

Richards, J. R., and P. D. Schnelle, "Perspectives on Industrial Reactor Control," *Chem. Eng. Prog.*, **84**(10), 32 (1988).

Schuler, H., and S. Zhang, "Real Time Estimation of the Chain Length Distribution in a Polymerization Reactor," *Chem. Eng. Sci.*, **40**, 1891 (1985).

Schuler, H., and S. Papadopoulou, "Real Time Estimation of the Chain Length Distribution in a Polymerization Reactor: II. Comparison of Estimated and Measured Distribution Functions," *Chem. Eng. Sci.*, **41**, 2681 (1986).

Schmidt, A. D., A. B. Clinch, and W. H. Ray, "The Dynamic Behavior of Continuous Polymerization Reactors: III. An Experimental Study of Multiple Steady States in Solution Polymerization," *Chem. Eng. Sci.*, **39**(3), 419 (1984).

Schmidt, A. D., and W. H. Ray, "The Dynamic Behavior of Continuous Polymerization Reactors-I: Isothermal Solution Polymerization in a CSTR," *Chem. Eng. Sci.*, **36**, 1401 (1981).

Schnelle, Jr., P. D., and J. R. Richards, "A Review of Industrial Reactor Control: Difficult Problems and Workable Solutions," *Chem. Process Cont.*, CPC III, M. Morari and T. J. McAvoy, eds., Elsevier, Amsterdam, 749 (1986).

Tsoukas, A., M. Tirrell, and G. Stephanopoulos, "Multiobjective Dynamic Optimization of Semibatch Copolymerization Reactors," *Chem. Eng. Sci.*, **37**, 1785 (1982).

Vogel, E. F., and T. F. Edgar, "An Adaptive Pole Placement Controller for Chemical Processes with Variable Dead Time," *Comput. Chem. Eng.*, **12**(1), 15 (1988).

Yu, C. C., and W. L. Luyben, "Design of Multiloop SISO Controllers for Multivariable Processes," *I&EC Proc. Des. and Dev.*, **25**, 498 (1986).

Manuscript received Oct. 4, 1988, and revision received Mar. 1, 1989.

See NAPS document no. 04686 for 36 pages of supplementary material. Order from NAPS c/o Microfiche Publications, P.O. Box 3513, Grand Central Station, New York, NY 10163. Remit in advance in U.S. funds only $12.55 for photocopies or $4.00 for microfiche. Outside the U.S. and Canada, add postage of $4.50 for the first 20 pages and $1.00 for each of 10 pages of material thereafter, $1.50 for microfiche postage.